Journal of the European Ceramic Society **11** (1993) 545–550

Grain and Grain Boundary Conduction in Zinc Oxide Varistors Before and After DC Degradation

T. Asokan* & R. Freer

Manchester Materials Science Centre, University of Manchester/UMIST, Grosvenor Street, Manchester M1 7HS, UK

(Received 20 July 1992; revised version received 5 November 1992; accepted 27 November 1992)

Abstract

ZnO-based varistors of typical commercial compositions have been studied before and after DC electrical degradation. Impedance spectroscopy was used to provide information about the behaviour of the ZnO grain and grain boundary regions. Degradation caused an increase in leakage current by a factor of 10, and a reduction in the Schottky barrier height by a factor of 2. The activation energy for grain conduction increased from 0·023 eV to 0·104 eV as a result of degradation, whilst that for grain boundary conduction decreased from 0·55 eV to 0·25 eV. The observed variation in the activation energies of bulk, grain and grain boundary regions are discussed in terms of positive interstitial Zn ion and negative oxygen ion migration in the grain boundary regions.

Auf ZnO basierende Varistoren mit einer typischen kommerziellen Zusammensetzung wurden vor und nach der Veränderung durch Anlegen einer Gleichspannung (Degradierung) untersucht. Die Impedanzspektroskopie lieferte Informationen über das Verhalten der ZnO-Körner und Korngrenzenregionen. Die Degradierung verursachte eine Zunahme des Restroms um einen Faktor 10 und eine Abnahme der Höhe der Schottky-Barriere um einen Faktor 2. Die Aktivierungsenergie der Kornleitfähigkeit nahm aufgrund der Degradierung von 0·023 auf 0·104 eV zu, während die Aktivierungsenergie für die Leitfähigkeit der Korngrenzen von 0·55 eV auf 0·25 eV abnahm. Die beobachtete Veränderung der Aktivierungsenergien des massiven Materials, des Korns und der Korngrenzenregionen wird bezüglich der interstitiellen positiven Zn- und negativen O-Ionenwanderung in den Korngrenzenregionen diskutiert.

Des varistances à base de ZnO, dans des compositions typiques du commerce, ont été étudiées avant et après dégradation sous courant continu. La spectroscopie d'impédance a été utilisée pour obtenir des informations quant au comportement des grains en ZnO et des joints de grains. La dégradation provoque une augmentation du courant de fuite d'un facteur 10 et un réduction de la hauteur de la barrière de Schottky d'un facteur 2. L'énergie d'activation de la conduction à travers le grain augmente de 0·023 eV à 0·104 eV après dégradation, tandis que celle correspondant à la conduction aux joints de grains diminue de 0·55 eV à 0·25 eV. Les variations observées pour les énergies d'activation en volume, des grains et des joints de grains sont discutées en terme de migration des ions Zn^{2+} interstitiels et des ions O^{2-} dans les joints de grains.

* Present address: Department of Electrical and Computer Engineering, University of South Carolina, Columbia, SC 29208, USA.

1 Introduction

Zinc oxide varistors are sintered polycrystalline devices that exhibit grossly non-linear current–voltage characteristics and good energy absorption capability.[1] These properties enable this class of materials to find wide application as circuit protection elements against transients and power overloads.[2,3] The superior properties of the varistor have led to several investigations from the viewpoint of conduction mechanism, microstructure and electrical properties.

The most serious problem encountered in the application of ZnO varistors is related to the phenomenon of degradation. The degradation process leads to increased power dissipation within the varistor and a concurrent rise in the varistor temperature, which may result in thermal runaway. The performance and life of ZnO varistors are therefore limited by degradation processes. The degradation behaviour of varistors has been studied

Journal of the European Ceramic Society 0955-2219/93/$6.00

under AC, DC and pulsed electric fields. Several mechanisms have been proposed to explain the observed degradation in terms of electron trapping, dipole orientation, ion migration and oxygen desorption.[4-11] However, it has been widely accepted that the degradation of ZnO varistors is associated with a deformation of the Schottky barriers, and this is believed to be caused primarily by ion migration in the depletion region of ZnO grains and grain boundary regions.[5,12] Since the degradation of ZnO varistors is believed to be a grain boundary phenomenon, most of the earlier studies were focused on the characteristics of the grain boundary phase. Nevertheless, if a process such as ion migration (caused by electrical stresses) is responsible for degradation, then it is likely that the characteristics of the ZnO grains and the grain boundary phase would vary simultaneously. The aim of the present study was therefore to provide an understanding of the characteristics of the grain and grain boundary phases in as-prepared and degraded varistor specimens by an AC impedance method. This technique permits unambiguous separation of the grain boundary and grain interior components of the conductivity for a polycrystalline sample.

2 Experimental Procedure

2.1 Sample preparation

Reagent grade (BDH Ltd, UK) powders of ZnO (87·425 wt%), Bi_2O_3 (6·00%), Sb_2O_3 (3·50%), CoO (0·55%), MnO_2 (0·70%), Cr_2O_3 (0·90%), NiO (0·90%) and $Al(NO_3)_3$ (0·025%) were mixed with deionised water in a vibratory ball mill for 10 h. The charge was dried, mixed with 2% polyvinyl alcohol and formed into discs of 15 mm diameter and 3 mm thickness using a single action uniaxial press, operating at 325 kg/cm^2. The green compacts were heated at 3°C/min, sintered at 1275°C for 2 h and cooled in the furnace to room temperature.

2.2 Characterisation

The densities of the sintered pellets were determined from mass and volume measurements. Phase analysis was carried out using a Philips X-ray diffractometer (PW 1380) with high density CuK_α radiation.

Samples to be used for microstructural studies were ground and polished down to 1 μm diamond paste. Scanning electron microscopy was performed on a Philips SEM 505 with an energy dispersive system (EDS) analytical facility, and specimens were carbon-coated prior to use.

Before electrical characterisation, metallic electrodes were applied to prepared (lapped) planar surfaces by coating with colloidal (air-drying) silver paint. Standard DC current–voltage (I–V) measurements were performed (using a stabilised DC power supply, Brandenburg 475R, in conjunction with precision digital multimeters, Fluke 8010A) in the current range up to 1 mA. The leakage current was estimated at the 80% $V_{1\,mA}$ level. Bulk resistance of the varistor samples was determined from I–V measurements at temperatures in the range 22°C to 153°C. The activation energy of the varistor was evaluated from plots of $\log R$ versus $1/T$ via the relationship:

$$R = R_0 \exp(E_A/kT) \quad (1)$$

where R is the resistance, R_0 is a constant, E_A is the activation energy, k is Boltzmann's constant and T the temperature (degrees Kelvin). The activation energy (E_A) in the above relationship is known to be a function of barrier height[13] as shown by:

$$E_A = \zeta + \phi_B - Td(\zeta + \phi_B)dT \quad (2)$$

where ζ is the Fermi level and ϕ_B is the barrier height.

AC impedance characteristics of the samples were determined as a function of frequency from 1 mHz to 10 kHz, over the temperature range 22°C to 153°C, by use of a computer-controlled frequency response analyser (Solartron 1250, Schlumberger Electronics Ltd, UK). The data were analysed in terms of impedance plots,[14] where the imaginary component of impedance (Z'') is plotted against the real component of impedance (Z') for each excitation frequency. An idealised impedance plot and the equivalent circuit of a ZnO varistor are shown in Fig. 1. The resistance of the grain (R_g) and the grain boundary (R_{gb}) may be derived from the intercepts of the semicircle and the real component (Z') axis as indicated in Fig. 1. Activation energies of the grain and grain boundary component conduction were determined from the respective Arrhenius plots of resistance as discussed in the case of bulk resistance.

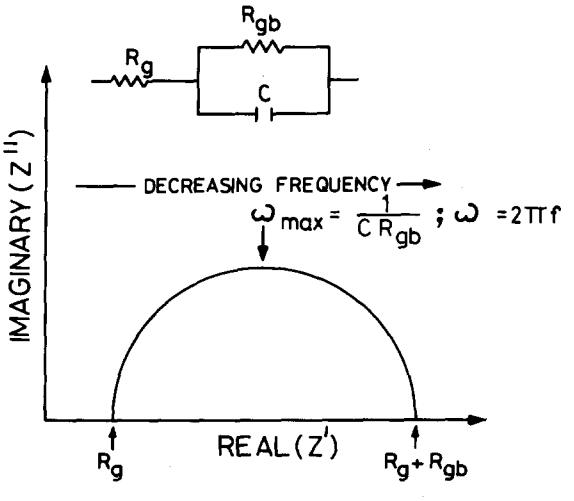

Fig. 1. The equivalent circuit and typical impedance plot of a ZnO varistor for the frequency range covered in this study. The capacitance shown refers to grain boundary barrier capacitance.

2.3 Sample degradation

Samples were degraded by subjecting them to a high DC current density (25 mA/cm^2) for 50 h at 150°C. During the test, the voltage was adjusted to maintain the constant current value. The DC and AC electrical characterisation of these samples, as already described, was performed before and after degradation.

3 Results and Discussion

3.1 Bulk properties of varistors

Sintered densities were approximately 96% of the theoretical value. X-Ray diffraction analysis did not reveal any differences between the phases present in the as-prepared and degraded samples. In both conditions, the samples comprised hexagonal ZnO, cubic Zn–Sb spinel and tetragonal β-Bi_2O_3 phases. The compositions of the ZnO-rich grains and the spinel ($Zn_7Sb_2O_{12}$) particles, determined by EDS analysis, are given in Table 1. The Bi_2O_3-rich grain boundary regions are too narrow to enable reliable analysis by these means.

The pre-breakdown current–voltage characteristics of the varistor before and after the application of electrical stress are shown (in terms of current density–electric field, i.e. J–E) in Fig. 2. The increase in leakage current after the application of electrical stress indicates that the varistors suffered a significant degree of degradation. It has been established[4,10,12] that conduction in the pre-breakdown region is mainly controlled by thermionic emission over the Schottky barrier. The observed increase in leakage current is believed to be caused by deformation of the Schottky barrier. It is also possible that formation of short circuit or conduction paths could lead to an increased leakage current without lowering the barrier. However, the formation and significance of the short circuit paths are not well understood. Arrhenius plots for sample bulk resistance, before and after degradation, are shown in Fig. 3. It may be seen that the application of electrical stress led to a reduction in the activation

Table 1. Typical compositions (obtained by EDS analysis) of phases in as-prepared and degraded ZnO varistors

Element (or as oxide)	*ZnO grain*		*Zn–Sb spinel*	
	Element (wt%)	*Oxide (wt%)*	*Element (wt%)*	*Oxide (wt%)*
Zn (ZnO)	79·61	99·10	43·79	54·51
Bi (Bi_2O_3)	—	—	—	—
Sb (Sb_2O_3)	—	—	24·89	29·80
Cr (Cr_2O_3)	—	—	4·24	6·20
Mn (MnO_2)	0·10	0·16	1·74	2·75
Co (CoO)	0·45	0·57	1·14	1·45
Ni (NiO)	0·14	0·18	4·17	5·31

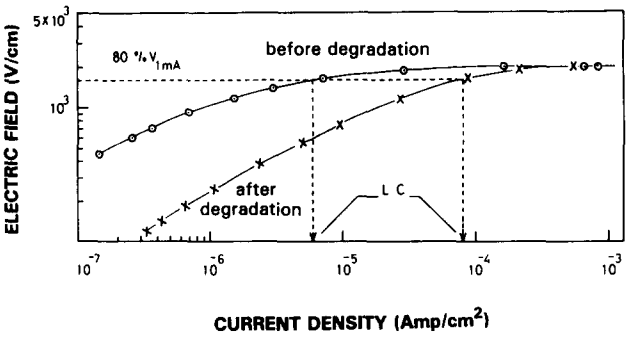

Fig. 2. Current density–electric field characteristics of ZnO varistor (⊙) before and (×) after degradation (LC = leakage current in each case).

energy ($E_A \approx \zeta + \phi_B$) from 0·57 eV to 0·28 eV. It has been shown that the barrier height (ϕ_B) of the varistors, estimated from the I–V characteristics, is reduced after degradation.[15] The observed reduction of the activation energy, in the present work, is therefore believed to be due primarily to the reduction in the potential barrier height.

In order to investigate the cause of activation energy reduction in the varistors, AC impedance measurements were also performed on as-prepared and degraded samples to reveal the characteristics of grain and grain boundary regions separately. Impedance plots for an as-prepared varistor at temperatures in the range 22–153°C are shown in Fig. 4. It may be observed that the total resistance ($R_g + R_{gb}$), based upon the low frequency intercept (right hand side) of the semicircle with the Z' axis, decreased with increasing temperature. The figure also shows that the frequency at which the maximum Z' value occurred (in each plot) increased with temperature. The grain resistance (R_g) was estimated from the high frequency intercept (left hand side) of the impedance plot with the Z' axis, and the grain

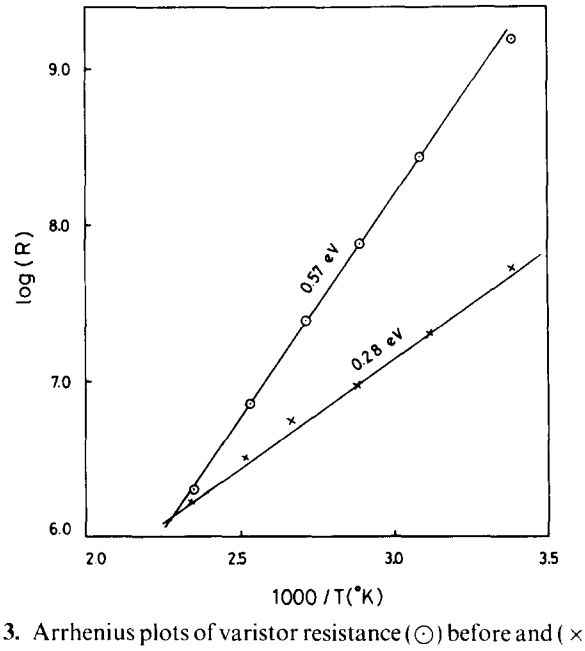

Fig. 3. Arrhenius plots of varistor resistance (⊙) before and (×) after degradation.

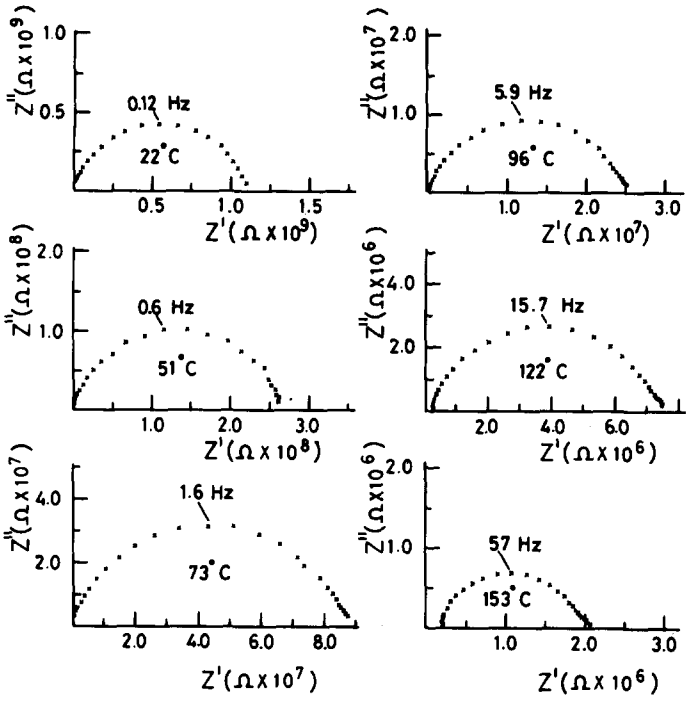

Fig. 4. Impedance plots of the varistor, before degradation, at temperatures from 22°C to 153°C.

boundary resistance (R_{gb}) was obtained from the difference between the low and high frequency intercept values (see also Fig. 1).

3.2 Characteristics of the ZnO grains

Arrhenius plots of ZnO grain resistance before and after degradation are shown in Fig. 5. As expected, the grain resistance decreased with increasing temperature, yielding activation energies of 0·023 eV and 0·104 eV for specimens before and after degradation respectively. It is interesting to note that the activation energy of the ZnO grains before degradation (0·023 eV), is significantly lower than the value (0·3 eV) reported for pure ZnO crystals.[16] The observed low activation energy (0·023 eV) of the ZnO grains before degradation therefore suggests

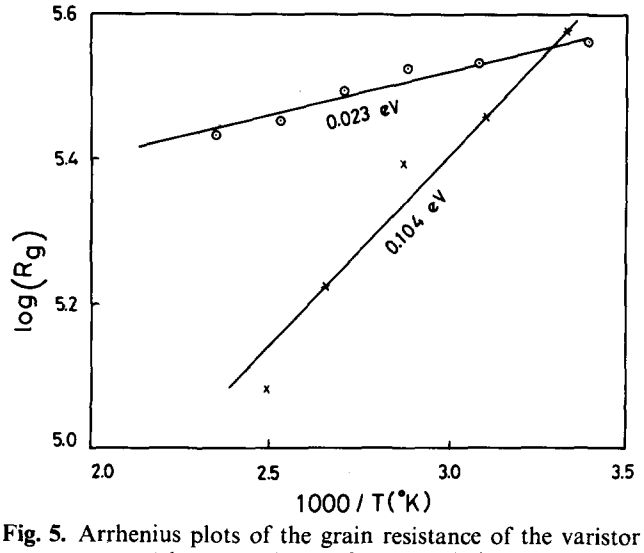

Fig. 5. Arrhenius plots of the grain resistance of the varistor (⊙) before and (×) after degradation.

that the grains in the ZnO varistor samples are not pure ZnO. This proposal is supported by the results of EDS analysis (Table 1) which indicate that the ZnO grains contain small amounts of CoO, MnO_2 and NiO. Indeed, the activation energy for the binary system ZnO–CoO is reported to be 0·05 eV.[17] The low activation energy (0·023 eV) for the varistor grains may therefore be attributed to the dissolution of additives such as CoO and possibly NiO in ZnO grains. However, a major cause of the reduction in the activation energy of the grains may be the presence of trivalent ions such as Al^{3+} and Cr^{3+} (added in the form of $Al(NO_3)_3$ and Cr_2O_3 to the charge) in the ZnO grains. This is because such trivalent impurities are known to form shallow donor defects, located at about 0·05 eV below the conduction band edge of ZnO.[18] The concentrations of the trivalent donor impurities in the ZnO grains, however, are believed to be very low (i.e. below the detection limit of analysis) as they were not observed by EDS analysis (Table 1).

Whilst the degradation process increased the activation energy for the ZnO grains from 0·023 eV to 0·104 eV (Fig. 5), the EDS analyses did not reveal any significant differences between the composition of the ZnO grains in the as-prepared and the degraded samples. The increase in the activation energy of ZnO grains is therefore believed to be associated with subtle changes in the composition of ZnO grains which are below the analytical detection limits.

It is possible to speculate that the increase in activation energy for the ZnO grains by degradation may have been caused by a process involving (i) the migration of trivalent impurities, and perhaps Zn interstitials, towards the grain boundary under the influence of an electric field, and (ii) the migration of oxygen atoms (from the grain boundary) towards the grain resulting in the oxidation of the impurities and Zn interstitials. There is, however, no evidence to support such a model and the process responsible for the increase in activation energy is yet to be identified.

3.3 Characteristics of the grain boundary

Arrhenius plots of the resistance of the grain boundary before and after degradation are shown in Fig. 6. In contrast to the behaviour of the ZnO grain, the activation energy of the grain boundary decreased after degradation from 0·55 eV to 0·25 eV. The observed decrease in the activation energy may be attributed to a change in the defect concentrations in the grain boundary phase.

The simultaneous change in the activation energies of grain and grain boundary regions (after degradation) may be due to the change in the concentration and nature of ionised charge carriers

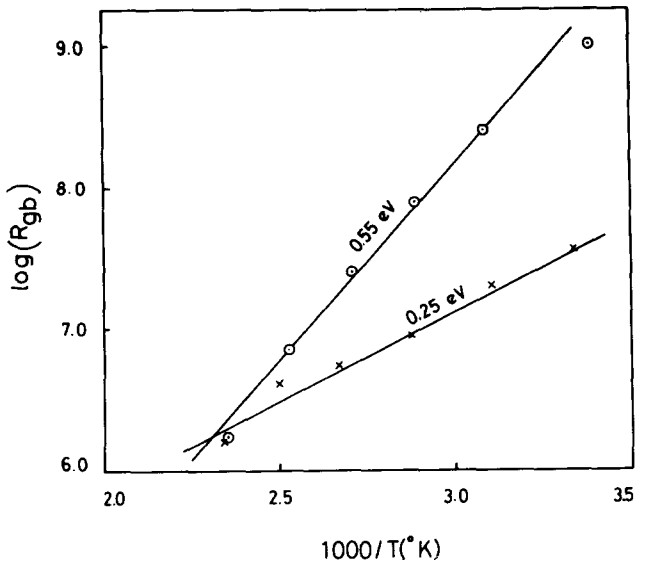

Fig. 6. Arrhenius plots of the grain boundary resistance of the varistor (⊙) before and (×) after degradation.

near the grain boundary regions. The depletion region, adjacent to the grain boundary interface, of ZnO varistors before degradation is known to be positively charged.[19,20] This is primarily due to the presence of mobile interstitial Zn ions (Zn_i^+ and Zn_i^{2+}) originating from the non-stoichiometric nature of ZnO and the spatially fixed (immobile) ions including the native oxygen vacancies such as V_O^+ and V_O^{2+} and ions based on the impurities such as Sb, Cr, Al and Bi. Under continuous or prolonged electrical stressing, the positive charges (e.g. Zn_i^+) are converted to neutral ions and accumulate at the grain interface, whilst the concentration of the mobile interstitial Zn ions in the depletion region is reduced.[19]

Simultaneously, the neutral oxygen present at the grain boundary regions would undergo ionisation to (O^- and O^{2-}) under the electric stress and migrate towards the depletion regions, whilst the Zn_i ions (from the depletion regions) migrate towards the grain boundary interface. A reaction between the Zn and oxygen ions can lead to the formation of neutral ZnO lattice.[19] Similar reactions involving other ions (Al^{3+}, Cr^{3+}, etc.) may also contribute to the increase in the grain activation energy. However, the migration of oxygen ions (originating at the grain boundary regions) towards the depletion region would cause depletion of oxygen at the grain boundary regions. The direct observation of oxygen depletion at the grain boundary regions of degraded varistors by Stucki *et al.*[21] support the above argument for the mechanism of oxygen ion migration towards the depletion region. The reduction in the grain boundary activation energy is therefore believed to be related to the oxygen depletion in the grain boundary regions.

The simultaneous increase in grain activation energy and decrease of grain boundary activation energy, after degradation, may thus be due to a process involving the simultaneous migration of positive ions such as Zn_i^+ and negative oxygen ions.

4 Conclusions

The increase of leakage current in ZnO varistors after the application of electrical stress is due to a reduction in the bulk activation energy which is a function of potential barrier height. The observed reduction of the bulk activation energy may be attributed to a simultaneous change in the activation energies of the grain and grain boundary phases. The activation energy of the ZnO grains was found to increase after degradation whereas the activation energy of the grain boundary decreased after degradation. The above change in the activation energies of grain boundary regions may be due to a simultaneous migration of negative oxygen ions and positive interstitial Zn ions.

Acknowledgements

The authors gratefully acknowledge the partial financial support provided by the Science and Engineering Research Council, access to the Frequency Response Analyser provided by Dr J. Scantlebury (Corrosion and Protection Centre, UMIST) and constructive comments on earlier versions of the manuscript by Dr D. A. Hall and Mr J. Fan (Manchester Materials Science Centre).

References

1. Matsuoka, M., Non-ohmic properties of ZnO ceramics. *Jpn. J. Appl. Phys.*, **10** (1971) 736–46.
2. Sakshaug, E. C., Kresge, J. S. & Miske, S. A., A new concept in station arrester design. *IEEE Trans. Power Appar. Syst.*, **PAS-96** (1977) 647–56.
3. Levinson, L. M. & Philipp, H. R., The physics of metal oxide varistors. *J. Appl. Phys.*, **46** (1975) 1332–41.
4. Eda, K., Iga, A. & Matsuoka, M., Degradation mechanism of non-ohmic ZnO ceramics. *J. Appl. Phys.*, **51** (1980) 2678–84.
5. Eda, K., Iga, A. & Matsuoka, M., Current creep in non-ohmic ZnO ceramics. *Jpn. J. Appl. Phys.*, **18** (1979) 997–8.
6. Shirley, C. G. & Paulson, W. M., The pulse-degradation characteristics of ZnO varistors. *J. Appl. Phys.*, **50** (1979) 5782–9.
7. Sato, K., Takada, Y., Maekawa, H., Ototake, M. & Tominaga, S., Electrical conduction of ZnO varistors under continuous DC stress. *Jpn. J. Appl. Phys.*, **19** (1980) 909–17.
8. Tominaga, S., Shibuya, Y., Fujiwara, Y., Imataki, M. & Nitta, T., Stability and long-term degradation of metal oxide arresters. *IEEE Trans. Power Appar. Syst.*, **PAS-99** (1980) 1548–56.
9. Moldenhauer, W., Bather, K. H., Bruckner, W., Hinz, D. & Buhling, D., Degradation phenomena of ZnO varistors. *Phys. Status Solidi (A)*, **67** (1981) 533–42.
10. Gupta, T. K., Carlson, W. G. & Hower, P. L., Current

instability phenomena in ZnO varistors under a continuous AC stress. *J. Appl. Phys.*, **52** (1981) 4104–11.
11. Takashi, K., Miyoshi, T., Maeda, K. & Yamazaki, T., Degradation of ZnO oxide varistors. In *Grain Boundaries in Semiconductors*, ed. J. H. Leamy, G. E. Pike & C. H. Seager. Elsevier, NY, 1982, pp. 399–404.
12. Gupta, T. K. & Miller, A. C., Improved stability of ZnO varistor via donor and acceptor doping at the grain boundary. *J. Mat. Res.*, **3** (1988) 745–54.
13. Pike, G. E. & Seager, C. H., Electronic properties of silicon grain boundaries. In *Advances in Ceramics*, Vol. 1, *Grain Boundary Phenomenon in Electronic Ceramics*, ed. L. M. Levinson & D. Hill. The American Ceramic Society, 1981, pp. 53–66.
14. Kilner, J. A., New techniques for studying mass transport in oxides. In *Kinetics and Mass Transport in Silicate and Oxide Systems (Materials Science Forum)*, Vol. 7, ed. R. Freer & P. F. Dennis. Trans. Tech. Publications, Switzerland, 1986, pp. 205–22.
15. Philipp, H. R. & Levinson, L. M., Degradation phenomena in ZnO varistors: a review. In *Advances in Ceramics*, Vol. 7, *Additives and Interfaces in Electronic Ceramics*, ed. M. F. Yan & A. H. Heuer. The American Ceramic Society, 1983, pp. 1–21.
16. Seitz, M., Hampton, F. & Richmond, W., Influence of chemisorbed oxygen on the AC electrical behaviour of polycrystalline ZnO. In *Advances in Ceramics*, Vol. 7, *Additives and Interfaces in Electronic Ceramics*, ed. M. F. Yan & A. H. Heuer. The American Ceramic Society, 1983, pp. 60–70.
17. Einzinger, R., Grain boundary phenomena of ZnO varistors. In *Grain Boundaries in Semiconductors*, ed. J. H. Leamy, G. E. Pike & C. H. Seager. Elsevier, NY, 1982, pp. 343–55.
18. Cardaro, J. F. & Shim, Y., Bulk electron traps in ZrO varistors. *J. Appl. Phys.*, **60** (1986) 4186–90.
19. Gupta, T. K. & Carlson, W. G., A grain-boundary defect model for instability/stability of ZnO varistor. *J. Mat. Sci.*, **20** (1985) 3487–500.
20. Gupta, T. K., Application of zinc oxide varistors. *J. Am. Ceram. Soc.*, **73** (1990) 1817–40.
21. Stucki, F., Bruesch, P. & Greuter, F., Electron spectroscopic studies of electrically active grain boundaries in ZnO. *Surf. Sci.*, **189/190** (1987) 294–9.